MOTT'S VARIABLE RANGE HOPPING MODEL FOR POLYPYRROLE-PAPAIN COMPOSITE POLYMER: INFLUENCE OF PAPAIN ENZYME ON COMPOSITE POLYMER

M. PANDEY

https://www.doi.org/10.59277/RJB.2024.2.03

Department of Physics, "K.M. Agrawal" College, Kalyan, Maharastra, India. 421301,
e-mail: drmunishpandey@yahoo.com

Abstract. Pure polypyrrole (ppy) doped with different weight percent of papain was synthesized by *in situ* polymerization. These different compositions of pyrrole and papain composite polymers were analyzed for direct current (DC) conductivity. The size of the particle calculated by using the Scherrer equation and Williamson-Hall (W-H) plot was found to be in the range of 15 nm – 20 nm. Activation energies evaluated by using Arrhenius plots show an increase in activation energy from base ppy to papain-ppy composite polymer. The activation energy was found to vary from 22.4 meV to 34.4 meV for papain-ppy composite. The experiment revealed that Mott's Variable Range Hopping model (VRH) for three dimensions (3D) applies to pure polypyrrole and papain-ppy composite. The density of states at the Fermi level $N(E_F)$ were found to be 2.7×10^{21} $eV^{-1}cm^{-1}$ for pure ppy and ranged from 0.3×10^{19} $eV^{-1}cm^{-1}$ to 0.8×10^{20} $eV^{-1}cm^{-1}$ for the composite polymer. The average hopping range and average hopping energy of pure ppy and composite polymers were also calculated.

Key words: polypyrrole (ppy), papain, VRH.

INTRODUCTION

Polypyrrole (ppy) is considered a versatile polymer capable of working as biocompatible and biodegradable material [12], which makes it suitable for fabricating conduits to guide nerve regeneration [10] and for other neural tissue applications [14]. Furthermore, ppy is a porous material with excellent optical and electrical properties characterized by a high conductivity/weight ratio [26]. Its chemical, electrical, and physical properties can be customized by incorporating antibodies, enzymes, and other biological materials. Ppy has the benefit of conjugated backbone with σ-bond and π-bond [1] possesses many excellent qualities like good chemical stability. It is easily and flexibly synthesized large quantities at room temperature. Ppy allows for a dynamic control of its properties by the

Received: February 2024;
in final form April 2024.

application of an electrical potential [6]. Ppy is applied in fuel cells [13], biosensors, and in neural tissue engineering [7].

Papain, also known as papaya proteinase I, is a proteolytic enzyme found in the unripe papaya; it assists in breaking down proteins into smaller fragments. Papain consists of a single polypeptide chain with three disulfide bridges and a sulfhydryl group necessary for its enzymatic activity. The molecular weight of papain is 23,406 Da [25]. The optimal pH and temperature stability for the better activity of this enzyme is 6.0–7.0 and 65 °C [9]. Electron beam irradiation shows an increase in papain's alternating current (AC) conductivity with temperature [19]. The thermal conductivity of papain was found in the range 0.58–0.62 W/m·K and the thermal diffusivity varied from 1.03×10^{-7} to 1.18×10^{-7} m^2/s in the temperature range of 20–40 °C [11].

Iron decorated ppy by using $FeCl_3$ as an oxidizing agent resulted in activation energy in the range of 9.3×10^{-3} eV to 57.005×10^{-3} eV [3]. The data obtained by four-probe measurements for hemoglobin-doped ppy revealed linear behavior as expected for a semiconductor [15]. The ppy nanotube prepared using the anionic azo dye assisted chemical oxidization method, liquid ammonia and ppy synthesized by using $FeCl_3$ as chemical oxidizing method was found to obey Mott's Variable Range Hopping (VRH) model in three dimensions [20, 23].

Chitosan grafted on an aniline-pyrrole copolymer had a conductivity of around 0.43937 (S cm^{-1}) [16]. In our previous paper, we studied the AC conductivity of papain–pyrrole composites and calculated the dielectric constant, dielectric loss, and tangent loss, which confirmed the presence of multi–relaxation time and charge transportation method by hopping between localized states [17]. We have also studied the antimicrobial activity of papain-ppy composite [18].

In this work, pure ppy was doped with different weight percent of enzyme papain. These composite polymers were characterized by X-ray diffraction analysis (XRD), field emission scanning electron microscopy (FESEM), Fourier transform infrared spectroscopy (FT-IR), and direct electric current (DC) conductivity. The activation energy and mode of transportation was also investigated with a special focus on DC applications.

MATERIALS AND METHODS

PREPARATION OF PPY AND PPY-PAPIN

Ppy-Cl powder was obtained by pyrrole polymerization in the presence of ferric chloride as an oxidant. An amount of 0.1 mol of $FeCl_3$ dissolved in 300 mL distilled water was stirred for 15 min; then 0.043 mol of pyrrole dissolved in 100 mL distilled water was added to the stirred mixture. The oxidant/pyrrole molar ratio has been discussed in our previous work [18]. Within one hour of moderate stirring, polymerization was carried out at room temperature.

To synthesize ppy-papain composite polymers, papain (0.1 g, 0.3 g and 0.5 g) various gram of papain was added to the previous mixture and the polymerization was allowed to proceed for 6 hours at room temperature. A black precipitate was obtained by filtering and washing with distilled water. The composites were dried at 60 ºC for 24 hours furthermore. For comparison, pure ppy was also prepared under the same reaction conditions.

RESULTS

The synthesized polymer samples were characterized using XRD, FESEM, FT-IR and DC conductivity analysis.

The XRD analysis was conducted at the X-ray crystallography laboratory at Sophisticated Analytical Instrument Facility (SAIF), Indian Institute of Technology, Bombay using a model Tr-60 diffractometer of Xenocs SAS with Model No. Xeuss 2.0, equipped with a graphite monochromator and rotating anode tube, operating with Cu, 50 kV, and 100 mA. XRD diffraction patterns were obtained in step scanning mode, $2\theta = 5–100°$.

The average chain separation (R) of ppy can be calculated from these maxima using the following relation [4]:

$$R = \frac{5\lambda}{8 \cdot \sin\theta} \tag{1}$$

where, R – chain separation, λ – X-ray wavelength, θ – diffraction angle. The average chain separation of pure ppy is 4.63 A.U. (atomic units).

The average crystallite size (D), as estimated from line broadening in X-ray diffraction, is expressed by Scherrer's formula:

$$D = \frac{k\lambda}{\cos\theta} \tag{2}$$

where k is the phase factor = 0.89, λ is the wavelength of X-rays = 1.54 Å. The average crystallite size (D) of pure ppy was found to be 15.57 nm and for the papain-ppy composites it ranged between 15 nm and 20 nm.

For pure ppy, the XRD analysis indicates a broad peak at $2\theta = 20.54^{o}$ [20]. The broad peaks, indicating some structural ordering of nanometric dimensions, are typical for nanostructured polymers with non-crystallin phase. The Williamson-Hall (W-H) plot is represented in Figure 1. The values obtained for ppy doped with various amounts of papain are shown in Table 1.

Figure 1 represents the W-H plot ($\beta \cos\phi$ versus $4 \sin\phi$, where β is the full width at half maximum and ϕ is the Bragg angle). The grain size calculated from W-H plot was found to be 15.566 nm, in good agreement with Scherrer's formula (Eq. 2).

Table 1

The values for 4 sin ϕ, and β cos ϕ for papain doped in ppy at lower concentration

No.	Papain doped in ppy (g)	4 sin ϕ	β cos ϕ
1	0	0.8308	0.0880
2	0.1	0.8652	0.0874
3	0.3	0.8308	0.0880
4	0.5	0.8352	0.0880

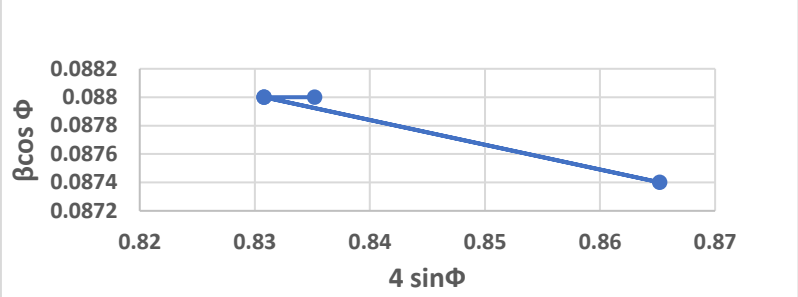

Fig. 1. W-H plot of papain-ppy composite doped with 0.1, 0.3, 0.5 g of papain.

The XRD patterns of ppy display a good fit using a monoclinic unit cell model and a semi crystalline pattern. The results obtained for papain-ppy composite polymers indicate that the structure of ppy is not affected by papain doping; the agglomeration is hampered and the crystallinity of papain-ppy composites is retained.

FESEM ANALYSIS

The FESEM analysis, shown in Figs. 2 and 3, reveals an increase in the size of granules as a result of doping the pure ppy with small amounts of papain. The average granule diameter of pure ppy is 160 nm, whereas doping with papain brings about an increase of the granule diameter to 200–260 nm.

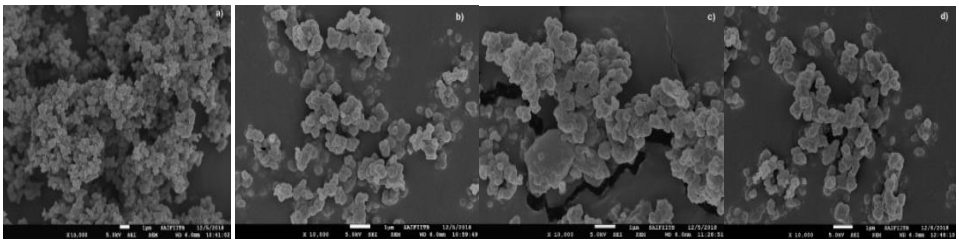

Fig. 2. FESEM analysis of a) pure ppy and papain-ppy composition containing b) 0.1 g papain; c) 0.3 g papain; d) 0.5 g papain.

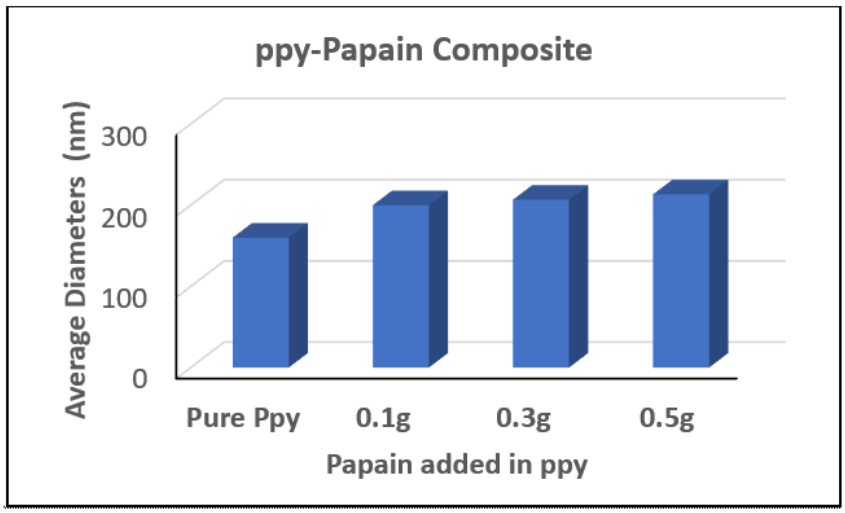

Fig. 3. Bar graph of the average diameter for a) pure ppy and papain-ppy composition containing b) 0.1 g papain; c) 0.3 g papain; d) 0.5 g papain.

Figure 2 reveals the uniform size and homogenous mixing of the papain-ppy composite. The agglomeration and formation of large size particles during synthesis of papain-ppy polymer might result from its non-polar character. The spherical particles of papain-ppy are attached to each other forming contiguous dots in the composite. The well-dispersed structure of the papain-ppy composite polymer could be beneficial for a uniform electrode morphology during charge-discharge processes.

FT-IR ANALYSIS

Fourier transform infrared spectra of the samples were obtained using a 3000 Hyperion Microscope with Vertex 80 FT-IR System (Bruker, Germany). The FT-IR analysis confirms the ppy polymerization during synthesis. It shows the functional groups existing in the pure ppy polymer as observed from FT-IR data listed in Table 2. The spectra observed in our study match with those published in literature for ppy and ppy doped with papain [4, 5, 8, 27].

The occurrence of the $–CONH_2$ I (1691 cm^{-1}), $–CONH_2$ II (1545 cm^{-1}), –C–S and S–S absorption bands conclude the occurrence of papain in the polypyrrole [22]. The broad IR band at 3424 cm^{-1} matches with the N–H stretching of secondary amide group [21]. The broad IR band is due to the hydrogen bonding between papain and ppy, which helps stabilizing the composite structure [4].

Table 2

The FT-IR analysis of pure ppy and ppy dopped with papain

No	IR Bands of pure ppy (cm^{-1})	IR Bands of ppy dopped with 0.1 g papain (cm^{-1})	IR Bands of ppy dopped with 0.3 g papain (cm^{-1})	IR Bands of ppy dopped with 0.5 g papain (cm^{-1})	Stretching/ Bending vibrations
1	–	422–430	422–430	503	S–S disulfide
2	609–669	610–671	612–679	604–679	S–S Str.
3	788	789	792	792	S–O R esters
4	917–965	917–965	922–965	920–966	–C–S Str
5	1045	1046	1047	1047	=C=S Str
6	1093	1093	1094	1095	–C–C str
7	1177	1178	1184	1182	–C–N Str.
8	1301	1298	1306	1301	=C–H Str
9	1468	1467	1474	1467	–C–N Str
10	1545	1547	1548	1549	–CONH– Str
11	1703	1691	1692	1708	–CO– Str
12	2853	2853	2853	2853	$–CH_2–$ Str.
13	2923	2923	2923	2923	–C–H Str.
14	3109	3096	3095	3097	$–CH_2–$ Str
15	3424	3422	3423	3405	N–H Str.

DC CONDUCTIVITY ANALYSIS

The DC conductivity (σ) for all the samples were recorded using an in-house built, temperature–controlled DC probe. The conductivity increased with temperature for all the samples. We also observed that adding small amounts (up to 0.3 g) of papain to ppy caused an increase in DC conductivity, whereas adding 0.5 g papain resulted in reduced conductivity.

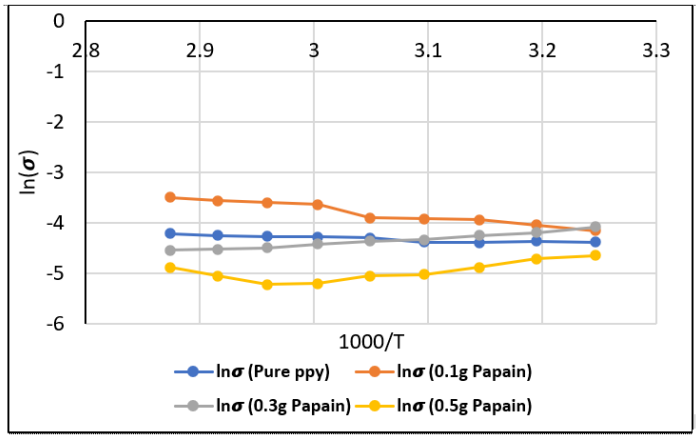

Fig. 4. Plot of ln (σ) *vs* 1000/T for pure ppy and ppy doped with small amounts of papain.

The plot of ln(σ) *vs* 1000/*T* for pure and papain composite shown in Figure 4 provides two slopes, namely regions I and II. This type of electrical conductivity behavior is in agreement with the Arrhenius model.

The activation energy is calculated by using the slopes derived by the plots [24]:

$$Activation\ energy = -slope \times \mathrm{k} \tag{3}$$

where k is Boltzmann's constant.

The activation energy values for pure ppy and papain-ppy in regions I and II are shown in Table 3. The results indicate that an increase in temperature causes an increase in disorder, which requires more hopping energy.

The added papain progressively widens the bipolaron band, which is associated with an increase in the activation energy (Table 3).

The conduction behavior of conducting polymers is explained by various theories; out of which Mott's Variable Range Hopping (VRH) model was the best fit to understand the mechanism of conduction in our case. Figure 5 plots ln(σ) *vs* $T^{(-1/4)}$ as given by Mott's VRH model which explains the charge carrier transport mechanism in an organic amorphous semiconductor. The linear fit of the plot of ln (σ) *vs* $T^{(-1/4)}$ indicates that the papain-ppy composite polymers obey Mott's law.

The experimental values of conductivity are plotted and r_0 the localization length, is taken as 10 A.U. for the monomer of dimensions ~ 3 A.U.

Table 3

The activation energy of pure ppy and papain ppy composite

Amount of papain doped in ppy (g)	**Activation energy (meV) Region I**	**Activation energy (meV) Region II**
0	21.5	34.4
0.1	49	66.3
0.3	91.3	43
0.5	133.5	229

MOTT'S VRH MODEL FOR THE CONDUCTION MECHANISM

The characteristic temperature associated with electron wave functions degree of localization (T_0), average hopping range (R) and average hopping energy (W) are calculated and given in Table 4 for pure and papain doped composite of ppy. For three dimensional (3D) parameters such as hopping range and average hopping energy are given below [28].

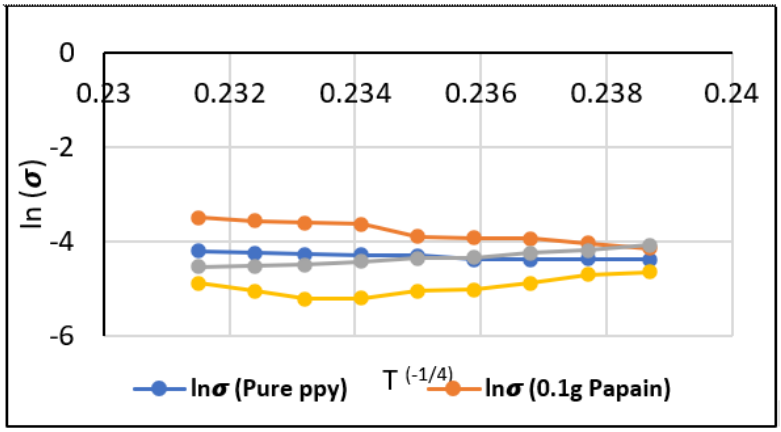

Fig. 5. Plot of ln (σ) *vs* $T^{(-1/4)}$ of pure and low papain doped composite of ppy.

$$T_0 = \frac{18}{r_0^3 \mathrm{k} N(E_\mathrm{F})} \tag{4}$$

$$R = \left[\frac{9r_0}{8\pi N(E_\mathrm{F})\mathrm{k}T}\right]^{1/4} \tag{5}$$

$$W = \frac{3}{4\pi R^3 N(E_\mathrm{F})} \tag{6}$$

where, r_0 is the electron wave function localization length, is taken as 10 A.U., k is the Boltzmann constant, T is temperature, and $N(E_\mathrm{F})$ is the density of states at the Fermi level.

The hopping parameters listed in Table 4 were calculated by using Eq. (5) and (6) along with the experimental data. The calculated values of density of states, average hopping range and average hopping energy are shown in Table 4 for different concentration of papain in ppy.

Table 4

Density of states, $N(E_F)$, average hopping range (R) and average hopping energy (W) of pure ppy and ppy doped with small amounts of papain using VRH model

Sample	**Pure ppy**	**0.1 g added papain**	**0.3 g added papain**	**0.5 g added papain**
T_0 (K)	77037	58.6×10^6	2.5×10^6	24×10^6
Density of states $N(E_\mathrm{F})$ ($\mathrm{eV^{-1}cm^{-1}}$)	2.8×10^{21}	0.3×10^{19}	0.8×10^{20}	0.87×10^{19}
Average hopping range R(Å)	14.87	82.3	36.2	63.1
R/r_0	1.487	8.23	3.62	6.31
Average hopping energy W (meV)	25.9	142	62.9	109.2

Remarkably, the ratio of R/r_0 is 1.4 for pure and 3.6 to 8.2 for papain-ppy composites. Since these values are greater than one, we conclude that the DC conduction in these materials is well described by the VRH model process.

The second condition for the validity of the VRH model is that the average hopping energy should be greater than k*T*. For the papain-ppy composites, *W* ranged from 62.9 meV to 142 meV, whereas for pure ppy it was smaller, close to the value of k*T*.

CONCLUSIONS

Papain-ppy composite polymers were prepared by the *in situ* polymerization method. The grain size was calculated from XRD readings, from a W-H plot and Scherrer's equation. FESEM analysis revealed that papain-ppy composite polymers are agglomerated and form large particles due to their non-polar character. FT-IR spectra confirmed the presence of papain in the synthesized composite polymers.

The experimental data on DC conductivity and Mott's VRH model calculations demonstrated a decrease in the density of states at the Fermi level from 2.8×10^{21} $eV^{-1}cm^{-1}$ for pure ppy to 0.3×10^{19} $eV^{-1}cm^{-1}$ – 0.8×10^{20} $eV^{-1}cm^{-1}$ for papain-ppy composite polymers.

Our results indicate that the sample containing 0.3 g of papain was characterized by the minimum energy required for a chemical reaction and minimum hopping energy required for conduction.

The average hopping range and the average hopping energy provided a validation of Mott's three-dimensional variable range hopping (VRH) model in the case of papain-ppy composite polymers.

Our study suggests that devices based on papain-ppy composites may be useful in the semiconducting industry.

Acknowledgements: My PhD student Richa Badlani and IIT, Mumbai, need to be acknowledged for timely support.

REFERENCES

1. ASPLUND, M., E. THANING, J. LUNDBERG, A.C. SADBERGORDQVIST, B. KOSTYSZYN, O. INGANAS *et al.*, Toxicity evaluation of PEDOT/biomolecular composites intended for neural communication electrodes, *Biomed. Mater.*, 2009, **4**, 1–12.
2. BASAVARAJA, C., N.R. KIM, E.A. JO, R. PIERSON, D.S. HUH, A. VENKATARAMAN, Transport properties of polypyrrole films doped with sulphonic acids, *Bull. Korean Chem. Soc.*, 2009, **30**(11), 2701–2706.
3. BASAVARAJA PATEL, B.M., M. REVANASIDDAPPA, D.R. RANGASWAMY, S. MANJUNATHA, Y.T. RAVIKIRAN, *Journal of Physics: Conference Series*, 2021, **2070**, 1–10.
4. CHEAH, K., M. FORSYTH, V.T. TRUONG, Ordering and stability in conducting polypyrrole, *Synth. Met.*, 1998, **94**, 215–219.

5. FU, Y., A. MANTHIRAM, Orthorhombic bipyramidal sulfur coated with polypyrrole nanolayers as a cathode material for lithium-sulfur batteries, *J. Phys. Chem*., 2012, **116(**16), 8910–8915.
6. GARNER, B., A.J. HODGSON, G.G. WALLACE, P.A. UNDERWOOD, Human endothelial cell attachment to and growth on polypyrrole-heparin is fibronectin dependent, *J. Mater. Sci. Mater. Med*., 1999, **10**, 19–27.
7. GHASEMI-MOBARAKEH, L., *et al*., Application of conductive polymers, scaffolds and electrical stimulation for nerve tissue engineering, *J. Tissue Eng. Regen. Med.*, 2011, **5**, e17–e35.
8. GRIMSLEY, G.R., C.N. PACE, *Spectrophotometric Determination of Protein Concentration, Current Protocols in Protein Science*, Chapter 3:3.1.1-3.1.9., John Wiley & Sons, Inc., 2001, doi: 10.1002/0471140864.ps0301s33. PMID: 18429266.
9. KLEIN, I.B., J.F. KIRSCH, The activation of papain and the inhibition of the active enzyme by carbonyl reagents, *J. Biol. Chem*., 1969, 2445928–5935.
10. KOTWAL, A., C.E. SCHMIDT, Electrical stimulation alters protein adsorption and nerve cell interactions with electrically conducting, *Biomaterials*, 2001, **22**,1055–1064.
11. KUROZAWA, L.E., K.J PARK, M.D. HUBINGER, F.E. XIDIEH MURR, P.M. AZOUBEL, Thermal conductivity and thermal diffusivity of papaya (*Carica papaya* L.) and cashew apple (*Anacardium occidentale* L.), *Braz. J. Food Technol*., 2008, **11**, 78–85.
12. LAKARD, B., L. PLOUX, K. ANSELME, F. LALLEMAND, S. LAKARD, M. NARDIN, *et al*., Effect of ultrasounds on the electrochemical synthesis of polypyrrole, application to the adhesion and growth of biological cells, *Bioelectrochemistry*, 2009, **75**, 148–157.
13. LEE, J.W., F. SERNA, J. NICKELS, C.E. SCHMIDT, Carboxylic acid-functionalized conductive polypyrrole as a bioactive platform for cell adhesion, *Biomacromolecules*, 2006, **7**, 1692–1695.
14. LEE, J.Y., C.A. BASHUR, A.S.GOLDSTEIN, C.E. SCHMIDT, Polypyrrole-coated electrospun PLGA nanofibers for neural tissue applications, *Bomaterials*, 2009, **30**, 4325–4335.
15. MEHTAB, S., M.G.H. ZAIDI, N. RANA, K. KHATI, S. SHARMA, Thermal and DC conducting behaviour of haemoglobin-doped polypyrrole, *Bull. Mater. Sci*., 2022, **45**, 162–169.
16. MISHRA, S.S., N.V. GHODKI, S. CHOPRA, S.A. PANDE, K.A. DESHMUKH, A.D. DESHMUKH, D.R. PESHWE, Synthesis and characterization of a novel conducting biopolymer chitosan grafted polyaniline-polypyrrole flexible copolymer, *Human Journals*, 2017, **8**, 104–111.
17. MUNISH, P., B. RICHA, AC conductivity and dielectric studies of polypyrrole-papain composite, *International Journal of Research – Granthalayah*, 2019, **7,** 332–338, https://doi.org/10.29121/granthaalayah.v7.i8.2019.681.
18. MUNISH, P., B. RICHA, Investigation of antibacterial activity of papain-polypyrrole composite against gram positive and gram-negative bacteria, *Invertis Journal of Science & Technology*, 2019, **12**(1), 1–4.
19. MUTHULAKSHMI, S., P. CHITHRALEKHA, M. BALAJI, G. SANJEEV, D. PATHINETTAM PADIYAN, Effect of exposure to electron beam irradiation in biopolymer papain and their electrical behavior, *Indian Journal of Pure & Applied Physics*, 2013, **51**, 33–38.
20. OTHMAN1, N., Z.A. TALIB1, A. KASSIM, A.H. SHAARI1, J.Y.C. LIEW, Electrical properties of polypyrrole conducting polymer at various dopant concentrations, *Journal of Fundamental Sciences*, 2009, **5**, 29–33.
21. OUYANG, J.Y., Y. F. LI, Great improvement of poly-pyrrole films prepared electrochemically from aqueous solutions by adding nonaphenol polyethyleneoxy ether, *Polymer*, 1997, **38**(15), 3997–3999.
22. PARTCH, R.E., S.G. GANGOLI, E. MATIJEVIC, W. CAI, S. ARAJS, Conducting polymer composites I: Surface-induced polymerization of pyrrole on iron (III) and cerium (IV) oxide particles, *Journal of Colloid and Interface Science*, 1991, **144(**1), 27–35.
23. PARVEEN, I.R., K. GOYAL, Effect of ammonia based deprotonation on the variable range hopping conduction in polypyrrole nanotubes, *Solid State Sciences*, 2020, **99**, 05984.

24. ROSAS-LAVERDE, N.M., A. PRUNA, D. BUSQUETS-MATAIX, Improving electrochemical properties of polypyrrole coatings by graphene oxide and carbon nanotubes, *Nanomaterials* 2020, **10**, 507, https://doi.org/10.3390/nano10030507
25. SMITH, E.L., J.R. KIMMEL, D.M. BROWN, Crystalline papain: II. Physical studies; the mercury complex, *J. Biol. Chem.*, 1954, 207533–549.
26. WALLACE, G.G., M. SMYTH, H.ZHAO, Conducting electroactive polymer-based biosensors, *Trends Analyt. Chem.*, 1999, **18**, 245–251.
27. WALLACE, G.G., G.M. SPINKS, L.A.P. KANE-MAGUIRE, P.R. TEASDALE, *Conductive Electroactive Polymers, Intelligent Materials Systems*, Second Edition 237, CRC Press, 2003.
28. YANG, C., P. LIU, Polypyrrole/conductive mica composites: preparation, characterization, and application in supercapacitor, *Synthetic Metals*, 2010, **160**, 768–773.